

Maximum total load effects in vehicle-bridge dynamic interaction problems for simply supported structures

D. Cantero^{1,2}, R. Karoumi², E.J. O'Brien³

¹Roughan & O'Donovan Innovative Solutions, Arena Road, Arena House, Dublin 18, Ireland

²Civil and Architectural Engineering, Royal Institute of Technology KTH, Stockholm, Sweden

³School of Civil, Structural and Environmental Engineering, University College Dublin, Dublin, Ireland

email: daniel.cantero@rod.ie, raid.karoumi@byv.kth.se, eugene.obrien@ucd.ie

ABSTRACT: This paper quantifies the underestimation of bending moment that results from exclusively considering the mid-span section of bridges when calculating vehicle-bridge dynamic interaction. A numerical model of a simply supported Euler-Bernoulli beam, traversed by a 1-DOF vehicle, is used to evaluate the differences. The simplicity of the model is justified by the additional insight that the results provide on the complex vehicle-bridge interaction problem. The results are presented using three dimensionless parameters that uniquely define the solution, taking into account the coupled system (vehicle and beam) frequencies and masses as well as the velocity of the passing vehicle. The results show that the overall maximum load effect occurs in the vicinity of the mid-span section and can be of significantly higher magnitude when compared to the maximum at mid-span.

KEY WORDS: Vehicle-Bridge Interaction, VBI, dynamics, bridge, truck, DAF.

1 INTRODUCTION

The most important result in Vehicle-Bridge interaction (VBI) problems is the maximum total load effect experienced by the structure, which consists of the combined contribution of static and dynamic effects. Bridge codes define Dynamic Amplification Factor (DAF) or similar parameters to obtain the total load effect from the static design load. In the case of simply supported structures, it is generally assumed that maximum bending moments and displacements occur at the mid-span section. Regarding the static contribution to the total load effect, this assumption is not correct when the traversing vehicle has an asymmetrical axle load distribution [1]. Furthermore, when considering the dynamic effects, this is generally not exact for any type of vehicle and axle configuration. In reality, the overall maximum load effect occurs in the vicinity of the mid-span section and can be of significantly higher magnitude when compared to the maximum at mid-span.

It is important to note that the phenomenon presented here is not exclusive to bridge dynamics that consider the coupling of the vehicle and bridge systems. Similar effects can be observed for the simpler situation where a beam is traversed by a moving constant load. A closed form solution exists [2] for such a case and this effect can easily be observed. However, it has been widely overlooked and its consequences on total dynamic effects generally neglected.

This paper aims to quantify the underestimation of total bending moment that results from exclusively considering the mid-span section of the structure. First, a simple vehicle-bridge interaction model is presented consisting of a simply supported Euler-Bernoulli beam, traversed by a 1-DOF vehicle. All possible solutions are uniquely defined by three dimensionless parameters that will be used throughout the document. It is possible from the presented results to extract conclusions for any particular bridge and vehicle configuration by calculating the corresponding parameters

based on the system properties. Additionally, section 3 offers an explanation on why the mid-span does not always feature the maximum load effect. Finally, particular emphasis is given to the influence of vehicle-to-bridge mass ratios and high speeds. For these cases, the results show that the mid-span load effects are significantly smaller than the actual maximum load effects experienced by the structure. These conditions are found in the interaction of high-speed trains traversing steel bridges.

2 NUMERICAL MODEL

The numerical model used in this study is presented Figure 1 and represents a simply supported bridge traversed by a moving vehicle. The structure is modelled as an Euler-Bernoulli beam using generalized coordinates and modal superposition [2]. The vehicle is approximated as a 1-DOF system composed of a mass connected to the beam by a spring. Table 1 lists all the variables of the described model. The coupled dynamic interaction between vehicle and bridge systems is achieved in an iterative manner [3] and solved numerically by direct integration, using the Newmark- β method [4]. Unless stated otherwise in the text, 20 modes of vibration are considered and the selected time step length is set to ensure that the solution is accurate up to the highest frequency considered.

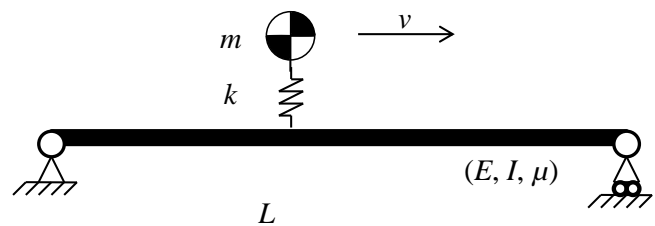


Figure 1. Sketch of Beam and moving 1-DOF oscillating mass.

Table 1: List of model variables

Variable	Description
m	Vehicle mass
k	Suspension vertical stiffness
v	Vehicle velocity
L	Beam length
E	Young's modulus
I	Second moment of area
μ	Mass per unit length

Equations (1) and (2) present the natural frequencies of the vehicle and the fundamental frequency of the beam respectively, both in Hz.

$$f_v = \frac{1}{2\pi} \sqrt{\frac{k}{m}} \quad (1)$$

$$f_b = \frac{\pi}{2L^2} \sqrt{\frac{EI}{\mu}} \quad (2)$$

The three dimensionless parameters used throughout this study are defined in Equations. (3-5). The Mass Ratio (MR) relates the vehicle mass to total structure's mass whereas the Frequency Ratio (FR) is the ratio between vehicle and bridge frequencies. The third dimensionless parameter is the Speed Parameter (SP) denoted in other studies as α [2] or S [3].

$$MR = \frac{m}{\mu L} \quad (3)$$

$$FR = \frac{f_v}{f_b} \quad (4)$$

$$SP = \frac{v}{2f_b L} \quad (5)$$

It is important to note that model configurations that feature the same three dimensionless parameters have the same dynamic response. Thus, the results presented in subsequent sections can be used to estimate the dynamics for a wide range of bridge and vehicle types. Generally, the main frequencies (bounce and pitch) of commercial vehicles range from 1 to 15Hz [5] and the fastest traversing speed corresponds nowadays to high-speed trains that have reached speeds over 500km/h [6]. Bridge frequencies generally range from 0.5 to 50Hz [7] and are normally many times heavier than the traversing vehicles. However, the mass ratio increases significantly in the case of long span steel railway bridges. Therefore, the range of the dimensionless parameters deemed appropriated in this study are 0.01 to 1 for MR and SP , and from 0.01 to 10 for FR .

The model presented here does not include any structural damping for the bridge or suspension viscous damping for the vehicle. It would be possible to consider both by introducing yet another dimensionless parameter, namely the damping parameter as presented in [2]. However, it was decided not to include it in order to limit the total number of dimensionless parameters. The intention of the results presented below is to give a general understanding of the phenomenon. It could be shown that the addition of damping leads only to a reduction of the dynamic factors presented in this paper while the studied phenomenon is still observed.

3 MAXIMUM LOAD EFFECT

The model described in previous section is used to determine the structural response for a configuration with parameters $(MR, FR, SP) = (0.1, 0.1, 0.1)$ as a representative example. The resulting total bending moment is normalised by dividing by the maximum static moment at mid-span as illustrated in Figure 2, in which the maximum corresponds to the Dynamic Amplification Factor (DAF) that for this particular case is found to be 1.044.

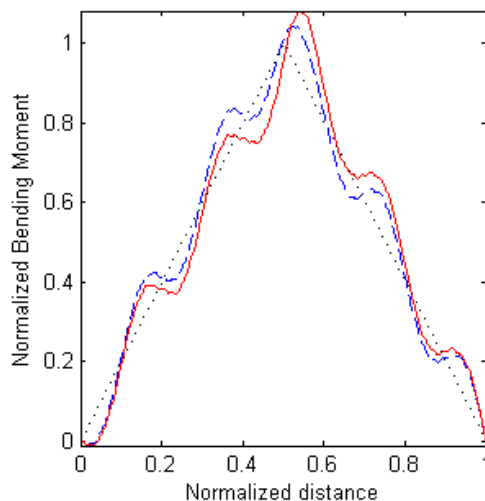


Figure 2. Normalized bending moment for $(MR, FR, SP) = (0.1, 0.1, 0.1)$; Mid-span static (dotted), mid-span total (dashed) and section with maximum total response (solid).

However, as the total response due to VBI is a complex problem, the maximum total bending moment value is commonly not located at exactly mid-span. Thus, Figure 2 also shows the normalized bending moment at the section with maximum total response where its maximum is referred to as FDAF, abbreviation derived from Full bridge length DAF [1]. This new dynamic amplification factor takes into account the whole bridge extent rather than just mid-span, and has a value of 1.081 in this particular case. It is important to note that both factors have been normalized by the same magnitude, namely the mid-span static bending moment. For completeness the definition of the mentioned amplification factors is given in Equations (6) and (7), where BM stands for Bending Moment.

$$DAF = \frac{Max. BM_{mid-span}}{Max. Static BM_{mid-span}} \quad (6)$$

$$FDAF = \frac{Max. BM_{full-length}}{Max. Static BM_{mid-span}} \quad (7)$$

A new magnitude is introduced now in order to readily compare both amplification factors. The value F is defined in Equation (8) as the difference between full length and mid-span dynamic amplification values. For the particular case presented in Figure 2, F has a value of 0.037, indicating that DAF should be increased in 3.7% to account for the dynamic effects of the bridge's full length.

$$F = FDAF - DAF \quad (8)$$

Figure 3 shows the bending moment amplification factors for a range of speed ratios. The DAF values feature a series of peaks and valleys, with some values below unity, indicating that in certain circumstances the total bending moment at mid-span is actually smaller than the static response. However, FDAF values are significantly different and feature values generally above 1. This illustrates that the total bending moment at some section of the bridge is greater than the mid-span static response during the vehicle crossing. FDAF is a better indicator of the dynamic effects for vehicle-bridge events. By definition, $FDAF \geq DAF$, which can be observed in Figure 3. Situations where both factors are the same indicate that the maximum load effect is taking place exactly at the mid-span section.

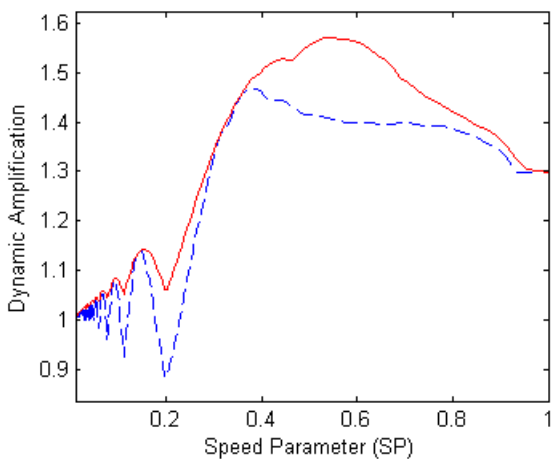


Figure 3. Bending moment DAF (dashed) and FDAF (solid) for constant parameters $(MR, FR) = (0.1, 0.1)$.

The dynamic response of a structure is the sum of the contributions from an infinite number of modes of vibration. Generally, in bridge engineering, the 1st mode is considered to be the most important, and even though the relative contribution of each subsequent mode rapidly diminishes, higher modes influence the total response too. It is precisely the contribution of the higher modes of vibration that leads to the differences between DAF and FDAF. Figure 4 shows the F values for models with increasing numbers of modes of vibration. When only the 1st mode of vibration is considered in the calculations, the maxima occur at mid-span. Thus F is always zero, indicating that there is no difference between amplification factors. However, as soon as the number of modes of vibration considered in the model is increased the maximum response does not necessarily occur at mid-span. The contribution of the higher modes leads to shifts in the location of the maximum load effect.

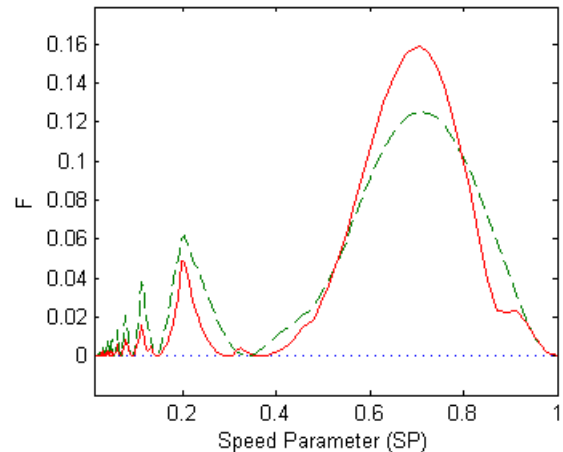


Figure 4. Bending moment F values considering models with 1-mode (dotted), 2-modes (dashed) and 3-modes (solid) and $(MR, FR) = (0.1, 0.1)$.

Also, it is interesting to show where in the beam the actual maximum bending moments occur. Figure 5 presents the location of the maxima for the same model configurations that have been presented in Figure 3. The maxima fluctuate significantly with the speed parameter and are found on both sides of the mid-span section. The range of variability is quite broad, and maximum load effects can occur anywhere between 30% and 70% of the bridge's span. The events that feature locations of 50% of L in Figure 5 correspond to the situations in Figure 3 where both amplification factors match.

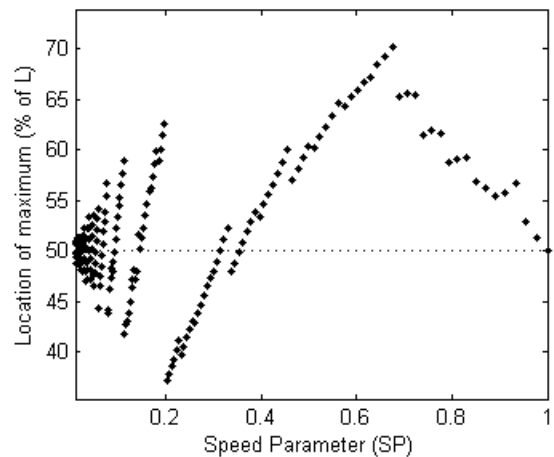


Figure 5. Location of maximum total bending moment for constant parameters $(MR, FR) = (0.1, 0.1)$.

4 RESULTS IN 3-PARAMETER SPACE

The previous section showed that maximum total load effect does not necessarily occur at the mid-span section, but only for a limited range of model configurations. This section aims to evaluate this phenomenon for a wider range of parameter values. For this, the model presented in Section 2 was used to find the solution for a wide range of the 3 dimensionless parameters. The intention of this study is to show the influence of various parameters and derive some general conclusions. However, due to the 3D nature of the results it is quite difficult to show all of them in detail. Therefore, following figures show only parts of the results with the

intention of presenting a general overview of the phenomenon.

Figure 6 and Figure 7 show slices through the 3D solution space where both figures have been represented with the same colour limits for ease of comparison. The colouring scheme is made of two distinct colour ranges – yellow/red/black and blue/green – to indicate values above and below unity.

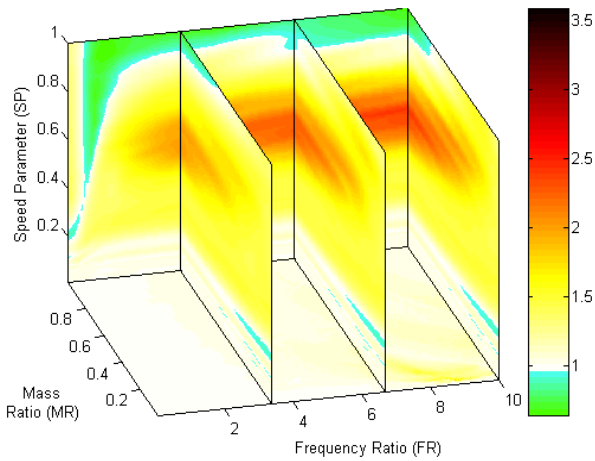


Figure 6. Slices of bending moment DAF solution in 3-parameter space

Figure 6 shows that a significant range of DAF solutions are below unity, whereas in Figure 7 only a small proportion of configurations indicate that the total bending moment is smaller than the mid-span static one. But most importantly, the direct comparison of both figures clearly shows that FDAF values are significantly bigger than DAF values and that both factors do not follow similar patterns. For instance, the maximum calculated DAF in Figure 6 is 2.408 while the maximum FDAF (Figure 7) reaches 3.583. The reader might argue that these very high amplification factors correspond to unrealistic situations. However, they indicate how different both indicators are and illustrate the necessity of an adequate factor to assess correctly the dynamics of bridges.

Additionally, it can be concluded that FDAF values generally tend to grow with increasing values of the dimensionless parameters. In contrast, DAF values might feature very small values for a combination of very high parameters, see $(MR, FR, SP) = (1, 10, 1)$ in Figure 6.

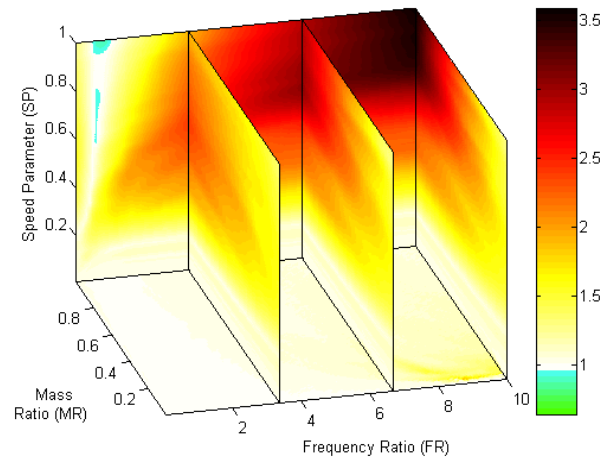


Figure 7. Slices of bending moment FDAF solution in 3-parameter space.

In order to clearly visualize the differences between both factors, Figure 8 presents the isosurfaces of F . Each surface represents the dimensionless parameters that give the same differences between amplification factors. The solution is rather complex but a clear trend can be observed. In general, for increasing dimensionless parameters the difference between FDAF and DAF increases. For instance, the red surface in Figure 8 corresponds to model configurations where the FDAF is equal to $DAF+2.6$. These occur only for very high dimensionless parameters which are very unlikely to be observed in reality. On the other hand, the light green surface covers a wider area and corresponds to much smaller (and more realistic) dimensionless parameters. However the F value for this surface is still 0.2. This means that DAF has to be increased by 20% (approximately) to allow for the correct dynamic assessment of the vehicle-bridge interaction.

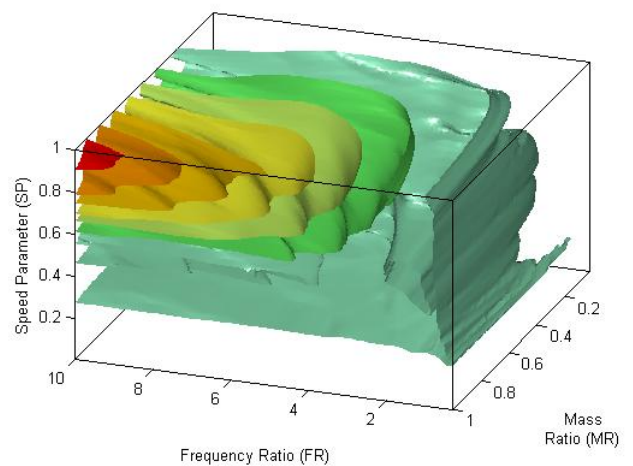


Figure 8. Bending moment F isosurfaces, for values of 0.2 (light green) to 2.6 in increments of 0.4.

Figure 9 gives the location where the actual bending moment occurs, expressed as a percentage of the beam's span. Note that now a smaller range of SP values are considered in order to being able to appreciate the great variability of these results. Again, two distinct colouring schemes are used to represent maxima occurring at both sides of the beam, where

lighter colours indicate the closeness to the mid-span section (50%). As in Section 3, the results fluctuate, and maxima can be found in both halves of the beam. It can be observed that the second half features more frequently in the maximum bending moment.

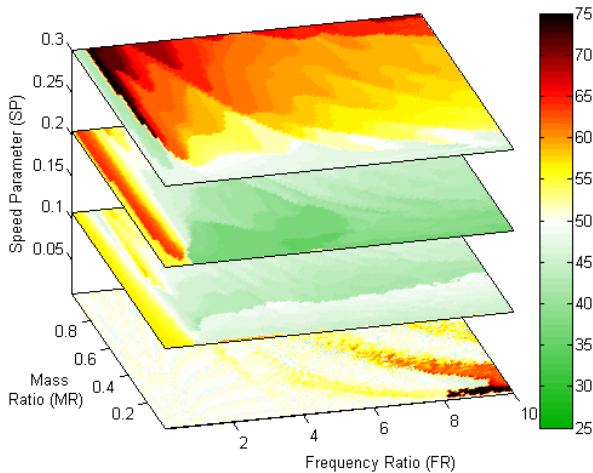


Figure 9. Slices of 3-parameter space results for location of maximum bending moment, in % of L .

5 EFFECT OF MASS RATIO

As shown in the previous section the results are quite complex and it is difficult to extract a general conclusion from them. One possibility is to focus only on the influence of the mass ratio, and consolidate the results on the other two dimensionless parameters.

Regarding the dimension related to the FR parameter, the results have been reduced by showing only the maximum along this dimension. It is believed that this is a reasonable approach because of the heterogeneity of the traffic traversing the bridge. In reality the mixture of vehicles will feature a wide range of frequencies. Thus, by taking the maximum factors over the FR values between 0.01 and 10, the resulting outcome is a (conservative) estimate of the dynamics due to the traffic fleet.

On the other hand, a different approach was adopted in reducing the results for the SP parameter which is related to the vehicle speed. At any given bridge, vehicles traversing the structure will travel with slightly different speeds. However, the distribution of these speeds has generally an upper bound. This limit might be related to the inherent maximum velocity achievable by the vehicle or due to a prescribed speed limit. Therefore, the results presented below are obtained by taking the maximum corresponding to FR up to a certain value. This has been termed here maximum-within-range. Thus, results for a maximum-within-range of $SP = 0.4$, are the maximum results corresponding to SP values from 0.01 to 0.4.

Figure 10 presents FDAF and DAF factors for the studied range of mass ratios, considering the maxima over SP and the maxima-within-range over FR . It is interesting to see that for smaller speeds (blue line), like those for road traffic, the amplification factors drastically reduce for increased mass ratios. This has been proven extensively for road bridges subject to traffic loads in many studies. Amongst many others this was shown using numerical simulations in [8] and experimental measurements in [9]. However, Figure 10 also

clearly shows that this is not the case when the considered range of speeds increases. For higher speeds, increasing the mass ratio reverses the trend observed for smaller speeds.

Additionally, Figure 10 shows that the differences between FDAF and DAF increase also with the range of speeds considered. For the case of maximum-within-range over SP of 0.1, i.e. smaller speeds (blue line), both results are very similar and are barely distinguishable. However, for higher speeds both amplification factors feature distinct values. The implications of these results are very relevant for railway bridges in high-speed lines where the total dynamic effects might be significantly bigger than those developed at mid-span.

6 CONCLUSIONS

This paper has presented the phenomenon of total load effects occurring at locations different than the mid-span section, which has been widely neglected in construction codes and related research. A simple numerical model is used in combination with three dimensionless parameters, to evaluate its consequences. It is clearly shown that the contribution of higher modes of vibration leads to shifts in the location of the maximum load effect. The alternative factor, FDAF is proven to be a better indicator of the dynamic effects in vehicle-bridge interaction problems. The results clearly show that FDAF values are significantly greater than DAF. It is observed that for low speeds the results are in accordance with current published conclusions indicating that both amplification factors are similar. However, in the event of higher speeds and mass ratios, it is shown that FDAF values can be significantly greater than its mid-span counterpart (DAF).

ACKNOWLEDGMENTS

The work presented in this paper was performed within the Long Life Bridges project, a Marie Curie Industry-Academia Partnerships and Pathways project, funded by the European Commission 7th Framework Programme (IAPP-GA-2011-286276).

REFERENCES

- [1] D. Cantero, A. González and E.J. O'Brien, *Maximum dynamic stress on bridges traversed by moving loads*, ICE Bridge Engineering, Vol. 162, No. 2, pp. 75-85, 2009.
- [2] L. Frýba, *Vibration of Solids and Structures under Moving Loads*, Thomas Telford, London, UK, third edition, 1999.
- [3] Y.B. Yang, J.D. Yau and Y.S. Wu, *Vehicle-Bridge Interaction Dynamics with applications to High-Speed Railways*, World Scientific, Singapore, 2004.
- [4] K.J. Bathe, *Finite Element Procedures*, Prentice Hall, Upper Saddle River, New Jersey, USA, 1996.
- [5] D. Cebon, *Interaction between Heavy Vehicles and Roads*, SAE International, 1993.
- [6] M. Givoni, *Development and impact of the modern high-speed train: A review*, Transport Reviews, Vol. 26, No. 5, pp. 593-611, 2006.
- [7] L. Frýba, *Dynamics of Railway Bridges*, Thomas Telford, London, UK, 2nd edition, 1996.
- [8] E.J. O'Brien, D. Cantero, B. Enright, A. Gonzalez, *Characteristic dynamic increment for extreme traffic loading events on short and medium span highway bridges*, Engineering Structure, Vol. 32, pp. 3827-3835, 2010.
- [9] A. Gonzalez et al., *Recommendations on dynamic amplification allowance, Assessment and rehabilitation of central European highway structures* ARCHES, Deliverable D10, 2009.

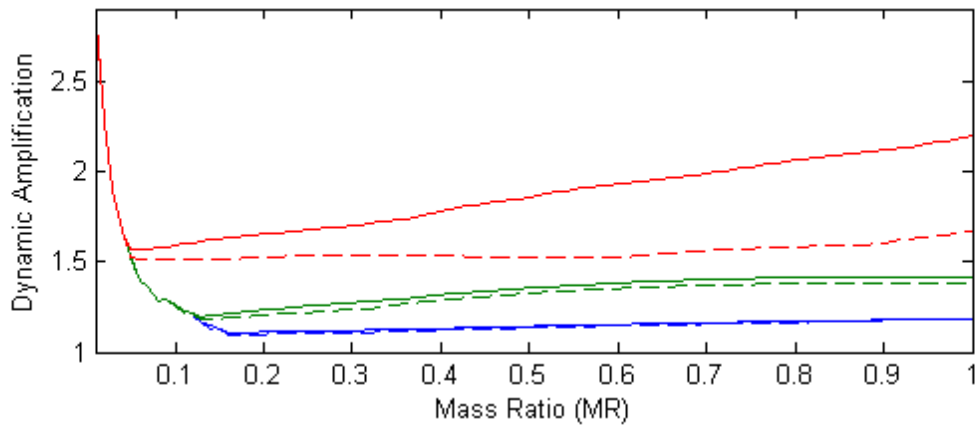


Figure 10. Bending moment dynamic amplification at mid-span (dashed) and full beam (solid), for maximum-within-range over SP of 0.1 (blue), 0.2 (green) and 0.4 (red).